# Structural Nucleotide Analogs Are Potent Activators/Inhibitors of Pancreatic β Cell KATP Channels: An Emerging Mechanism Supporting Their Use as Antidiabetic Drugs

Domenico Tricarico, Jean-François Rolland, Gianluigi Cannone, Antonietta Mele, Valentina Cippone, Antonio Laghezza, Giuseppe Carbonara, Giuseppe Fracchiolla, Paolo Tortorella, Fulvio Loiodice, and Diana Conte Camerino

*Departments of Pharmacobiology (D.T., J.-F.R., G.C., A.M., V.C., D.C.C.) and Medicinal Chemistry (A.L., G.C., G.F., P.T., F.L.), Faculty of Pharmacy, University of Bari, Bari, Italy*

## ABSTRACT

The 2H-1,4-benzoxazine derivatives are novel drugs structurally similar to nucleotides; however, their actions on the pancreatic β cell ATP-sensitive $K^+$ (KATP) channel and on glucose disposal are unknown. Therefore, the effects of the linear/branched alkyl substituents and the aliphatic/aromatic rings at position 2 of the 2H-1,4-benzoxazine nucleus on the activity of these molecules against the pancreatic β cell KATP channel and the Kir6.2ΔC36 subunit were investigated using a patch-clamp technique. The effects of these compounds on glucose disposal that followed glucose loading by intraperitoneal glucose tolerance test and on fasting glycemia were investigated in normal mice. The 2-n-hexyl analog blocked the KATP ($IC_{50}$ = $10.1 \times 10^{-9}$ M) and Kir6.2ΔC36 ($IC_{50}$ = $9.6 \times 10^{-9}$ M) channels, which induced depolarization. In contrast, the 2-phenyl analog was a potent opener (drug concentration needed to enhance the current by 50% = $0.04 \times 10^{-9}$ M), which induced hyperpolarization. The ranked order of the potency/efficacy of the analog openers was 2-phenyl > 2-benzyl > 2-cyclohexylmethyl. The 2-phenylethyl and 2-isopropyl analogs were not effective as blockers/openers. The 2-n-hexyl (2–10 mg/kg) and 2-phenyl analogs (2–30 mg/kg) reduced and enhanced the glucose areas under the curves, respectively, after glucose loading in mice. These compounds did not affect the fasting glycemia as is observed with glibenclamide. The linear alkyl chain and the aromatic ring at position 2 of the 1,4-benzoxazine nucleus are the determinants, which confer the KATP channel blocking action with glucose-lowering effects and the opening action with increased glucose levels, respectively. The opening/blocking actions of these compounds mimic those that were observed with ATP and ADP. The results support the use of these compounds as novel antidiabetic drugs.

## Introduction

Drugs that target the pancreatic β cell ATP-sensitive $K^+$ (KATP) channels are used in glucose/insulin dysmetabolisms (Gribble and Reimann, 2003; Jahangir and Terzic, 2005; Arnoux et al., 2010; Ashcroft, 2010). This channel is a complex that is composed of the sulfonylureas receptor type-1 (SUR1) and the inwardly rectifying $K^+$ channel (Kir6.2) sub-units (Seino and Miki, 2003). The SUR1 subunit carries the binding sites for the KATP channel openers and blockers (Babenko et al., 2000; Moreau et al., 2005). KATP channel blockers are prescribed to individuals who are in the diabetes-aged population and who display impaired glucose-induced insulin release (Nourparvar et al., 2004). These drugs belong to the following distinct classes: the first-generation sulfonylureas (chlorpropamide, tolbutamide, and tolazamide), which are low-affinity ligands of the SUR1 subunit that cause the release of insulin at micromolar concentrations; the second- (glipizide and glyburide) and third-generation sulfonylureas (glimiperide and acetohexamide), which

**ABBREVIATIONS:** KATP, ATP-sensitive $K^+$; AUC, area under the curve; BPDZ-73, 7-chloro-3-isopropylamino-4H-1,2,4-benzothiadiazine-1,1-dioxide; $DE_{50}$, drug concentration needed to enhance the current by 50%; HEK, human embryonic kidney; KCO, KATP channel openers; Kir6.2, inwardly rectifying $K^+$ channel; NBF2, nucleotide binding fold-2; TMD2, second transmembrane domain; SUR1, sulfonylureas receptor type-1; BPDZ-62, N-(3,3-dimethylbutan-2-yl)-1,1-dioxo-4H-pyrido[4,3-e][1,2,4]thiadiazin-3-amine; NNC-55-0118, 6-chloro-1,1-dioxo-N-propan-2-yl-4H-thieno[3,2-e][1,2,4]thiadiazin-3-amine; NN414, 6-chloro-N-(1-methylcyclopropyl)-1,1-dioxo-4H-thieno[3,2-e][1,2,4]thiadiazin-3-amine; NNC-55-0462, 6-chloro-3-(1-methylcyclobutyl)amino-4H-thieno[3,2-e]-1,2,4thiadiazine 1,1-dioxide.

**2**     **Tricarico et al.**

are high-affinity and slowly reversible ligands of the SUR1 subunit that act at nanomolar concentrations; and the glinides, which lack the sulfonylurea moiety and include repaglinide, nateglinide, and meglitinide, which are high-affinity SUR1 ligands, exhibit a rapid onset/offset action compared with that of the sulfonylureas (Gribble and Reimann, 2003).

The sulfonylureas and the glinides are being investigated for use in the treatment of hypotension that results from septic shock, ischemic trauma, and neonatal diabetes (Koster et al., 2005; Flechtner et al., 2006; Pearson et al., 2006; Flanagan et al., 2007; Mlynarski et al., 2007; Simard et al., 2008; Ashcroft, 2010). Severe hypoglycemia, weight gain, and cardiovascular side effects limit their use in special populations (Zünkler, 2006). Long-term exposure of β cells to sulfonylureas induces a reduction in the insulin content and the number of KATP channels (Takahashi et al., 2007). Therapeutic concentrations of sulfonylureas and high doses of glinides induce the apoptosis of β cells, β cell lines, or cell lines that express the recombinant KATP channel subunits, and these effects are mediated by SUR1 (Maedler et al., 2005; Hambrock et al., 2006). Glibenclamide also causes atrophy of the skeletal muscles (Tricarico et al., 2010). It has been proposed that sulfonylurea-induced atrophy contributes to the loss of β cell mass that characterizes the progression of diabetes (Takahashi et al., 2007).

The pancreatic KATP channel openers (KCOs) belong to the benzothiadiazine class, which includes the diazoxide and thiadiazine-1,1-dioxide derivatives, such as N-(3,3-dimethylbutan-2-yl)-1,1-dioxo-4H-pyrido[4,3-e][1,2,4]thiadiazin-3-amine (BPDZ-62), 7-chloro-3-isopropylamino-4H-1,2,4-benzothiadiazine-1,1-dioxide (BPDZ-73), 6-chloro-3-(1-methylcyclobutyl)amino-4H-thieno[3,2-e]-1,2,4thiadiazine 1,1-dioxide (NNC-55-0462), 6-chloro-1,1-dioxo-N-propan-2-yl-4H-thieno[3,2-e][1,2,4]thiadiazin-3-amine (NNC-55-0118), and 6-chloro-N-(1-methylcyclopropyl)-1,1-dioxo-4H-thieno[3,2-e][1,2,4]thiadiazin-3-amine (NN414); cyanoguanidines; nitropyrazoles; and 4-sulfamoylphenylbenzamides (Hansen, 2006; Carosati et al., 2007). Diazoxide is prescribed for the treatment of acquired and tumor-related hypoglycemia, familial hyperinsulinemia hypoglycemia in infancy, and polycystic ovary syndrome (Jahangir and Terzic, 2005; Hussain, 2007; Arnoux et al., 2010). Diazoxide protects the β cells from sulfonylurea-induced apoptosis, high glucose, and cytokine-induced toxicity, which preserves the insulin stores (Teshima et al., 2003). In skeletal muscle, diazoxide prevents glibenclamide-induced atrophy (Tricarico et al., 2010). The SUR1-selective openers have been proposed to treat epilepsy and neurodegenerative disorders, in which the SUR1/Kir6.2-Kir6.1 subunits play a role (Carosati et al., 2007). However, diazoxide is unselective, which can lead to hypotension and tachycardia, severe fluid retention, sedation, and weakness.
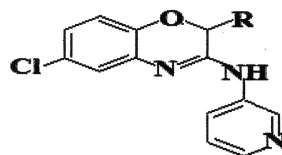
The 2H-1,4-benzoxazine derivatives have emerged as novel KATP channel modulators. In the presence of ATP, these molecules display KCO activity, whereas in the absence of the nucleotide they display a blocking action (Tricarico et al., 2003, 2008). These compounds have structural similarities with ATP and ADP molecules. A conformational analysis showed that the planar area of the 2H-1,4-benzoxazines overlaps that of the adenine nucleotide tri- and diphosphates. The electronic distribution profile of this area is also similar to that of the adenine nucleotides, which were reached by electrons; this result suggests that these compounds share a common ATP/ADP interaction interface on the receptor sites (Tricarico et al., 2008). No data are available regarding the effects or possible dual actions of these nucleotide analogs on the pancreatic β cell KATP channel or glucose disposal in normal mice.

The molecular determinants that were responsible for the activity of the 2H-1,4-benzoxazine derivatives toward the β cell KATP channels and the Kir6.2ΔC36 subunit that was expressed in HEK293 cells therefore were investigated using patch-clamp techniques. The influence of the linear/branched alkyl chain substituents at position 2 of the 2H-1,4-benzoxazine nucleus on the biological activity of the molecules against the KATP channel was evaluated by testing the effects of the 2-n-hexyl- and 2-isopropyl-1,4-benzoxazine derivatives. The influence of an aromatic/aliphatic ring on the biological activity of the molecules against the KATP channels was evaluated by testing the effects of 2-cyclohexylmethyl-, 2-phenyl-, 2-benzyl-, and 2-phenylethyl-1,4-benzoxazines (Fig. 1). The drug effects on glucose disposal and fasting glycemia in normal mice also were investigated.

## Materials and Methods

**Pancreatic β Cells and tsA201 Cells Expressing the Kir6.2ΔC36 Channel.** All of the experiments were conducted in accordance with the Italian Guidelines for the Use of Laboratory Animals, which conform with the European Community Directive that was published in 1986 (86-609-EEC). The method of pancreatic β cell preparation has been described previously (Rolland et al., 2002, 2006). Sixty to 100 islets per culture from two mice were prepared. The islets were identified by optical morphological inspection and insulin secretion. The β cells were identified by their spherical form/size, capacitance of $8 \pm 3$ pF (number of cells = 45) (α or δ



**2H-1,4 benzoxazine nucleus**

| Compound | R |
|---|---|
| *n*-hexyl | H₃C— (hexyl chain) |
| Isopropyl | H₃C—CH(—CH₃) |
| Phenyl | (phenyl ring) |
| Benzyl | (benzyl group) |
| 2-(phenyl)-ethyl | (phenylethyl group) |
| Cyclohexyl-methyl | (cyclohexylmethyl group) |

**Fig. 1.** Chemical structures of the newly synthesized 2-H-1,4-benzoxazine derivatives that were tested on the pancreatic KATP channels.

AQ: A

F1,AQ:B

tapraid3/zpt-pt/zpt-pt/zpt00212/zpt9675d12z | xppws | S=1 | 12/30/11 | 18:29 | 4/Color Figure(s): 9 | Art: 185835 | Input-JHG

K$^+$ Channel Modulators and Pancreatic $\beta$ Cells   **3**

cells have a lower capacitance), current/membrane potential response to high or low glucose concentrations (see step 1 below), current responses to diazoxide or tolbutamide (see step 5 below), and insulin secretion in response to increasing concentrations of external glucose (Fig. 2). Studies on the Kir6.2ΔC36 channel in HEK293 cells used Kir6.2ΔC36 (mouse) that was inserted in the mammalian expression vector pCDNA3, which was provided generously by Professor F. M. Ashcroft (Department of Physiology, Anatomy and Genetics, University of Oxford, Oxford, UK). The HEK293 cells were cotransfected with 4 µg of DNA that encoded the channel and a lower amount of plasmid DNA that encoded the CD8 receptors using Lipofectamine 2000 and Opti-MEM (Invitrogen, Carlsbad, CA).

**Insulin Secretion.** Triplicates of the eight islets were cultured in 10% fetal calf serum and 1 ml of Krebs-Ringer-bicarbonate buffer with HEPES medium with 2 mg/ml bovine serum albumin and 5 mM glucose overnight in air (5% $CO_2$) at 37°C before the experiments. An equilibrium period of 120 min with 0 mM glucose of the islets was performed; this was followed by a period of incubation with different glucose concentrations (0.5–10 mM) for 60 min in 5% $CO_2$ at 37°C to evaluate insulin secretion in the medium. The islets were sonicated to facilitate insulin extraction. The insulin concentrations in the sonicate and the medium were determined with the use of rat/mouse insulin enzyme-linked immunosorbent assays (Millipore Corporation, Billerica, MA) (Fig. 2C).

**Solutions and Drugs.** For the perforated or conventional whole-cell recordings, the extracellular bath solution contained 140 mM NaCl, 4.8 mM KCl, 2.5 mM $CaCl_2$, 1.2 mM $MgCl_2$, 10 mM HEPES (pH 7.4), and various concentrations of glucose. The electrical contact was established by adding amphotericin B to the pipette solution (stock, 60 mg/ml in dimethyl sulfoxide; final concentration, 300 µg/ml). For the perforated patch mode, the pipette solution contained 70 mM $K_2SO_4$, 10 mM NaCl, 10 mM KCl, 3.7 mM $MgCl_2$, and 5 mM HEPES (pH 7.1); 5 mM $K_2ATP$ and 1 mM $Na_3GTP$ were added to the pipette solution for the conventional whole-cell mode. $K_2SO_4$ was replaced by an equimolar concentration of KCl using $BaCl_2$. For the inside-out recordings, the bath solution contained 140 mM KCl, 5 mM EGTA, and 20 mM HEPES (pH 7.2). The intrapipette solution contained 140 mM KCl, 2.6 mM $CaCl_2$, 1 mM $MgCl_2$, 10 mM EGTA, and 20 mM HEPES (pH 7.4). The synthesis of the 2*H*-1,4-benzoxazine derivatives has been described previously (Fig. 1) (Tricarico et al., 2003). All of the other chemicals were purchased from Sigma-Aldrich (St. Louis, MO).

**Patch-Clamp Experiments.** The drug experiments were performed using the patch-clamp methodology in the voltage-clamp mode (perforated whole-cell, conventional whole-cell, and inside-out configurations), and the current-clamp mode was performed using Clampex software (Molecular Devices, Sunnyvale, CA) (Rolland et al., 2006; Tricarico et al., 2008).

The pancreatic $\beta$ cells were perfused continuously with different solutions at a flow rate of 2 ml/min, and the changes in the currents were monitored. The patch perforation and whole-cell configurations were evaluated by monitoring the changes in the current capacitance and access resistance, which were 22 ± 6 and 30 ± 3 MΩ in the whole-cell and perforated patch experiments, respectively. The protocol that was applied for the identification of $\beta$ cells and the drug test was as follows:

1. external glucose 10, 6, or 3 mM and $NaN_3$ (5 mM)
2. external glucose 10, 6, or 3 mM and $NaN_3$ (5 mM) (control)
3. external glucose 10, 6, or 3 mM, $NaN_3$ (5 mM), and drugs
4. washout
5. external glucose 10, 6, or 3 mM, $NaN_3$ (5 mM), and diazoxide (2.5 × 10$^{-4}$ M) or tolbutamide (5 × 10$^{-4}$ M).
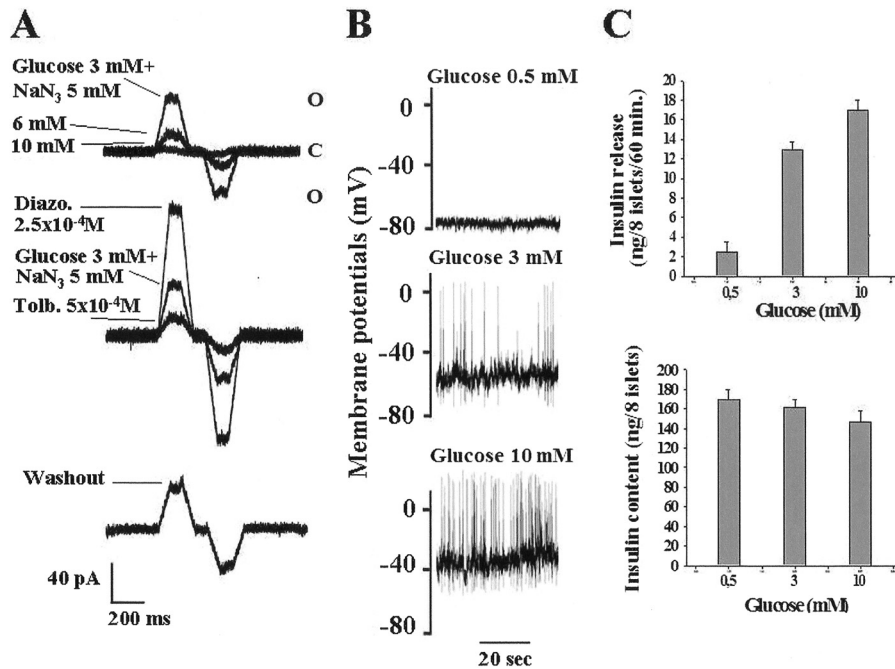


**Fig. 2.** Protocols used for the identification of the pancreatic $\beta$ cells and islets. A, sample traces of KATP currents were recorded using a perforated patch-clamp in the whole-cell mode from $\beta$ cells that first were exposed to a bath solution that was enriched with 10 mM glucose followed by 3 mM glucose and 5 mM $NaN_3$ or 6 mM glucose solutions. The currents were recorded during pulses of ±20 mV (Vm) from a holding potential of −70 mV (Vm) (O indicates the open channel levels as upward or downward deflections of the current record, and C indicates the closed level). The decrease in the external glucose concentration led to the enhancement of the whole-cell currents. The responses of the current after the application of diazoxide (Diazo.) or tolbutamide (Tolb.) in the presence of 3 mM glucose and 5 mM $NaN_3$ and a washout of the drug solution are represented. Diazoxide increased the whole-cell current, whereas tolbutamide reduced it, and their effects were reversible. B, sample traces of the membrane potentials versus time from the $\beta$ cells that were exposed to different concentrations of glucose were recorded in the current-clamp mode. The exposure of the $\beta$ cells to increasing external glucose led to cell depolarization and firing. C, the insulin secretion was induced by low or high levels of external glucose and the residual insulin content in the islets. Batches of eight islets were incubated with different concentrations of external glucose for insulin release; the insulin content of the islets was evaluated after ethanol and HCl extraction. Each bar is the mean ± S.E. of three values.

No more than two drug concentrations per cell were tested. The drug solutions were applied to the patches using a fast perfusion system (AutoMate Scientific, Berkeley, CA).

It should be noted that the low patch-clamp performance in 10 mM glucose can mask the blocking actions of the investigated drugs. In this experimental condition, we indeed measured a very low residual current that did not allow us to quantify the blocking action of the drugs on this parameter.

**Intraperitoneal Glucose Tolerance Test.** This test was performed on six groups of 8-week-old nondiabetic mice after an overnight fast as described previously (Rolland et al., 2006). The noncyclic 2$H$-1,4-benzoxazine derivatives (0.2, 2, 10, or 30 mg/kg), the 2-phenyl analog (2, 10, and 30 mg/kg), glibenclamide (0.2 and 2 mg/kg), and diazoxide (2 mg/kg) were dissolved in a solution that contained polyoxyethylene sorbitan monooleate (10%) and 0.9% NaCl (90%).

This treatment was followed with evaluations at 24 h and 14 days postdose to identify any possible intolerability of the single intraperitoneal injection of the compounds. The primary end points that were evaluated were mild symptoms, such as piloerection, sedation, and weakness. The secondary end points were severe symptoms, such as abdominal cramps, convulsion, and moribundity.

**Analysis of the Results and Statistics.** The off-line analysis was performed using Clampfit, Fetchan, pSTAT (Molecular Devices), and Excel (Microsoft, Redmond, WA). The mean current (single-channel current $\times$ open probability $\times$ number of channels) was evaluated in an excised patch as the digital average of the sampled points, whereas the single-channel conductance (pS) was evaluated as the slope of the current-voltage relationship. The experiments are illustrated by the traces, means, or representative results that were obtained from at least three different cultures. The concentration-response data were fitted by an equation that described the interaction of the ligand with one inhibitory site, as in the case of the 2-hexyl analog data, or by the sum of two equations that described the interaction of the ligand with two sites that exerted opposite actions, as in the case of the 2-cyclic analog data (Tricarico et al., 2008). The stimulatory component can be described by the following term: $(I_{drug} - 1) \times 100 = A_{max}/(1 + (DE_{50}/[Drug])^n)$; and the inhibitory component can be described by the following term: $(I_{drug} - 1) \times 100 = I_{max}/(1 + ([Drug]/IC_{50})^n)$. $I_{max}$ indicates the percentage maximal inhibition of the pancreatic KATP channel and Kir6.2ΔC36 channel currents that were caused by the compounds. $A_{max}$ indicates the percentage maximal activation of the KATP currents that was produced by the compound under investigation. $DE_{50}$ indicates the concentration of the drug that was needed to enhance the current by 50%, which was calculated with respect to the current levels that were recorded in the absence of drugs. $IC_{50}$ is the concentration of the drug that is needed to reduce the current by 50%, which was calculated with respect to the current levels that were recorded in the absence of the drugs. $N$ indicates the number of sampled cells per drug, whereas $n$ indicates the slope factor of the curves. The algorithms of the fitting procedures that were used were based on a Marquardt least-squares fitting routine. The data analysis and the plot were performed using SigmaPlot software (Systat Software, Inc., San Jose, CA). The data are expressed as the mean $\pm$ S.E. The statistical significance of the differences between the means was assessed by the Student's $t$ test. The differences were considered significant for $P < 0.05$.

## Results

**Effects of 2$H$-1,4-Benzoxazine Derivatives on the Native Pancreatic β Cell KATP Channels of Mice and on the Kir6.2ΔC36 Channel That Was Expressed in HEK293 Cells.** We first evaluated the effects of 2-isopropyl and 2-$n$-hexyl analogs on the β cell KATP channel in the presence of 3, 6, or 10 mM glucose in the bath using the

perforated and/or conventional whole-cell patch clamp mode. The exposure of the patches to a solution that was enriched with the 2-linear alkyl chain analog ($10^{-10}$–$10^{-4}$ M) inhibited the KATP channel currents of β cells in the perforated and conventional whole-cell modes in a concentration-dependent manner (Fig. 3, A, B, D, and F). In the perforated whole-cell patch mode, at $-50$ mV (Vm) the current was reduced from $42 \pm 3$ pA in the control to $18 \pm 3$ pA after the application of a $10^{-7}$ M concentration of the drug (Fig. 3A). In the conventional whole-cell mode, at $-50$ mV (Vm), the current was reduced from $38 \pm 2$ pA in the control to $25 \pm 2$ and $19 \pm 3$ pA after the application of $10^{-8}$ and $10^{-7}$ M concentrations of the drug, respectively (Fig. 3B). In the intact cell, the inhibitory effect of this compound was fully reversible after a 5-s washout of the drug solution. The 2-$n$-hexyl analog (from $10^{-10}$ to $10^{-4}$ M) reduced the Kir6.2ΔC36 channel currents that were recorded in the HEK293 cells pulsed to a test potential of $-100$ mV (Vm) using the conventional whole-cell patch mode. This drug reduced the Kir6.2ΔC36 current from $-980 \pm 22$ pA in the control to $750 \pm 36$ and $200 \pm 21$ pA in the presence of $10^{-8}$ and $10^{-6}$ M concentrations of the drug, respectively (Fig. 3C). In the presence of 6 mM glucose, in the perforated patch mode, the current was reduced from $21 \pm 3$ pA in the control to $10 \pm 2$ pA after the application of a $10^{-7}$ M concentration of the blocker (Fig. 3D). In the perforated patch mode, the 2-branched alkyl chain analog failed to affect the KATP currents in the presence of either 3 mM glucose and 5 mM NaN$_3$ or 6 mM glucose (Fig. 3, A and D), and it did not affect the Kir6.2ΔC36 channel. In the presence of 10 mM glucose, the 2-$n$-hexyl and 2-isopropyl analogs ($10^{-8}$–$10^{-6}$ M) did not significantly affect the currents (Fig. 3E). A $5 \times 10^{-4}$ M concentration of tolbutamide almost fully reduced the currents in 3 and 6 mM glucose, and it showed a mild effect in 10 mM glucose (Fig. 3, A, D, and E). The mild blocking effect of tolbutamide that was observed in 10 mM glucose may be related to the low patch-clamp performance that was described under *Materials and Methods*.

The concentration-response curve analysis showed that at $-50$ mV (Vm), in 3 mM glucose, and using the perforated patch method, the $IC_{50}$ of the 2-hexyl analog that was present in the range of concentrations tested was $10.1 \pm 3 \times 10^{-9}$ M; in the conventional whole-cell patch mode, the $IC_{50}$ was $9.8 \pm 2 \times 10^{-9}$ M in the β cells and $9.6 \pm 1 \times 10^{-9}$ M in the cell line that was expressing the Kir6.2ΔC36 channel (Fig. 3F; Table 1). These values were not statistically different.

The coapplication of $10^{-9}$ M glibenclamide and the 2-$n$-hexyl analog ($10^{-8}$ M) to the β cells caused a $53 \pm 4\%$ reduction in the currents (number of cells = 3) in the conventional whole-cell patch mode. Glibenclamide ($10^{-9}$ M) and the 2-$n$-hexyl analog ($10^{-8}$ M) caused a $25 \pm 3\%$ (number of cells = 2) and $27 \pm 4\%$ (number of cells = 3) reduction in the currents, respectively. The KATP current indeed was reduced from $39 \pm 2$ pA in the control to $29 \pm 2$ pA in the presence of $10^{-9}$ M glibenclamide and $16 \pm 2$ pA after the coapplication of $10^{-9}$ M glibenclamide and $10^{-8}$ M of the 2-$n$-hexyl analog to the cell (Fig. 3B).

Conversely, in the perforated patch-clamp experiment and in the presence of 3 or 6 mM external glucose, the 2-phenyl-, 2-benzyl-, and 2-cyclohexylmethyl-1,4-benzoxazine derivatives enhanced the KATP currents at sub-nanomolar concentrations. In 3 mM glucose and 5 mM NaN$_3$, the percentage activations of the currents were $91.2 \pm 4\%$ (number of cells =

| tapraid3/zpt-pt/zpt-pt/zpt00212/zpt9675d12z | xppws | S=1 | 12/30/11 | 18:29 | 4/Color Figure(s): 9 | Art: 185835 | Input-JHG |

K$^+$ Channel Modulators and Pancreatic β Cells     **5**
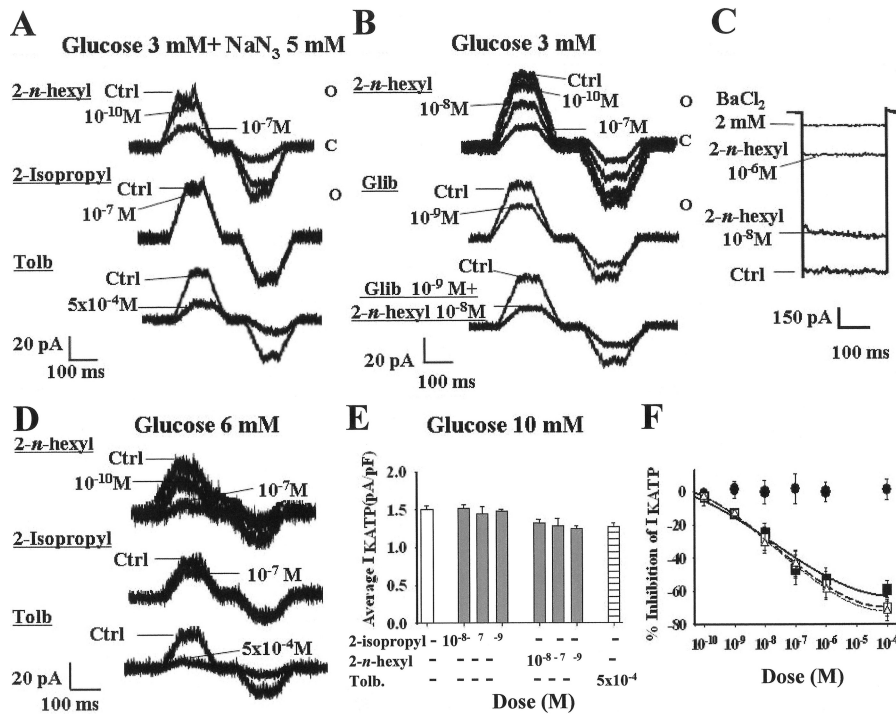
**Fig. 3.** Effects of the 2-isopropyl- and 2-n-hexyl-1,4-benzoxazine derivatives on the KATP currents of the mouse pancreatic β cells and on the Kir6.2ΔC36 channel that was expressed in the HEK293 cells. Sample traces of the whole-cell KATP currents were recorded in the pancreatic β cells during pulses of ±20 mV (Vm) from a holding potential of −70 mV (Vm); the measurements were performed in the absence (control, Ctrl) or presence of drugs and with different external glucose concentrations using the perforated patch mode or the conventional whole-cell mode. The Kir6.2ΔC36 current was recorded in the HEK293 cells using the conventional whole-cell patch during a pulse of −100 mV (Vm). O indicates the open channel levels as upward or downward deflections of the current record, and C indicates the closed level. Increasing concentrations of the same drug are indicated on the corresponding current traces. A and B, at −50 mV (Vm) using the perforated patch mode in 3 mM glucose and 5 mM NaN$_3$ (A) and the conventional whole-cell patch mode (B), the 2-n-hexyl analog, which showed a threshold concentration of $10^{-10}$ M in both experimental conditions, inhibited the KATP current with similar efficacy. B, the coapplication of glibenclamide and the 2-n-hexyl analog to the β cells enhanced the channel block induced by the 2-hexyl analog. C, the 2-n-hexyl analog reduced the Kir6.2ΔC36 current, and BaCl$_2$ caused a further reduction in the channel currents. D, in 6 mM glucose, the 2-n-hexyl analog inhibited the KATP current of the β cell, which showed a threshold concentration of $>10^{-10}$ M. Tolbutamide (Tolb.) almost fully reduced the currents (A and D). E, the average β cell KATP current density versus the 2H-1,4-benzoxazine or tolbutamide concentrations ($10^{-8}$–$10^{-6}$ M) in 10 mM glucose. Each bar represents the mean ± S.E. of the current data from three cells. F, the concentration-response relationships of the KATP currents of the β cells versus the 2-isopropyl- (black circles) and 2-n-hexyl-1,4-benzoxazine (black squares) concentrations that were constructed at −50 mV (Vm) in 3 mM glucose using the perforated patch or the whole-cell patch mode for 2-n-hexyl analog (white squares). F, the concentration-response relationship of the Kir6.2ΔC36 currents versus the 2-n-hexyl analog concentration (white triangle) constructed at −100 mV (Vm) using the conventional whole-cell patch mode. Each experimental point represents the mean ± S.E. of the percentage inhibition of the KATP currents versus the drug concentrations of three cells; no more than two drug concentrations per cell were tested.

12) and 58.2 ± 6% (number of cells = 7) for $10^{-10}$ M of the 2-phenyl and 2-benzyl analogs, respectively. The currents that were measured at −50 mV (Vm) in 3 mM glucose and 5 mM NaN$_3$ were 40 ± 4 pA in the control and 65 ± 4 and 75 ± 5 pA with 0.7 × $10^{-10}$ and $10^{-10}$ M concentrations of the 2-phenyl analog, respectively; they were 61 ± 5 pA after the application of a $10^{-10}$ M concentration of the 2-benzyl analog (Fig. 4A). For the 2-phenyl and 2-benzyl analogs in 6 mM glucose, the activations were 96.1 ± 8% (number of cells = 4) and 61.2 ± 6% (number of cells = 4), respectively. The currents that were measured at −50 mV (Vm) in 6 mM glucose were 19.5 ± 3 pA in the control and 38 ± 4 and 32 ± 4 pA after the application of a $10^{-10}$ M concentration of the 2-phenyl and 2-benzyl analogs, respectively (Fig. 4B). In 3 mM glucose and 5 mM NaN$_3$ or 6 mM glucose, $10^{-7}$ M of the 2-phenyl- analog produced 17 ± 5% (number of cells = 12) and 20 ± 6% (number of cells = 3) reductions of the respective currents with respect to those of the controls, whereas the 2-benzyl analog produced 21 ± 4% (number of cells = 7) and 16 ± 5% (number of cells = 4) increases in the currents, respectively (Fig. 4, A and B). The 2-cyclic analogs appeared to be more effective in 6 mM glucose than 3 mM glucose, but

the observed differences were not statistically significant. However, in 10 mM glucose, the 2-cyclic derivatives ($10^{-9}$–$10^{-7}$ M) were less effective (Fig. 4C).

Bell-shaped concentration-response curves were observed with the effective 2-cyclic-1,4-benzoxazine derivatives in the native pancreatic β cells (Fig. 4A). All of the effective 2-cyclic-1,4-benzoxazine derivatives showed a reduced efficacy at concentrations of $>10^{-9}$ M. The 2-phenyl analog ($10^{-11}$–$10^{-6}$ M) was the most potent and effective compound in enhancing the KATP currents; its DE$_{50}$ was 0.04 ± 0.01 × $10^{-9}$ M (Fig. 3A; Table 1). The 2-cyclohexylmethyl analog ($10^{-10}$–$10^{-7}$ M) was less effective, whereas the 2-phenylethyl analog ($10^{-10}$–$10^{-7}$ M) did not affect the KATP current (Fig. 4, A and C).

The percentage activations of the currents by 2.5 × $10^{-4}$ M diazoxide were 220 ± 12, 400 ± 20, and 150 ± 11% (number of cells = 6) with respect to the controls in 3 mM glucose and 5 mM NaN$_3$, 6 mM glucose, and 10 mM glucose, respectively. A 2.5 × $10^{-4}$ M concentration of diazoxide in 3 mM glucose enhanced the whole-cell currents from 43 ± 5 pA in the control to 140 ± 7 pA and in 6 mM glucose from 27 ± 6 pA and 137 ± 9 pA in the control and after the application of the drug to the cells, respectively (Fig. 4, A and B). Significant

**6**　Tricarico et al.

TABLE 1

Fitting parameters of the concentration-response curves of the 2H-1,4-benzoxazine derivatives versus the pancreatic β cell KATP channel currents, which were recorded using the perforated or conventional whole-cell patch clamp, and the Kir6.2ΔC36 channel currents that were expressed in HEK293 cells, which were recorded using the conventional whole-cell patch clamp

These compounds are the 2$H$-1,4 benzoxazine derivatives that contain linear alkyl or cyclic groups at position 2 of the benzoxazine nucleus. The range of concentrations that was tested for each compound is given in parentheses. The concentration-response curves for these drugs were constructed in the presence of 3 mM glucose in the bath in the pancreatic β cells using the perforated (glucose and 5 mM $NaN_3$) and/or conventional whole-cell recordings ($^a$) and in the HEK293 cells that were transfected with the Kir6.2ΔC36 channel subunit using the conventional whole-cell recordings ($^a$). Kir6.2ΔC36 is the truncated Kir6.2 subunit that was expressed in the cell line, whereas KATP is the native ATP-sensitive potassium channel of the pancreatic β cell.

| | Compounds | KATP | | | | | Kir6.2ΔC36 | | |
|---|---|---|---|---|---|---|---|---|---|
| | | $I_{max}$ | $A_{max}$ | $DE_{50}$ | $IC_{50}$ | $n$ | $I_{max}$ | $IC_{50}$ | $n$ |
| | | % | % | $10^{-9}$ M | $10^{-9}$ M | | % | $10^{-9}$ M | |
| Linear | 2-$n$-Hexyl ($10^{-10}$–$10^{-4}$ M) | $-59.1 \pm 5$ $n = 10$ $-68 \pm 5^a$ $n = 12$ | | | $10.1 \pm 3$ $n = 10$ $9.8 \pm 2^a$ $n = 12$ | $-0.5 \pm 0.1$ $n = 10$ $-1 \pm 0.1^a$ $n = 12$ | $-69.9 \pm 5^{*,a}$ $n = 4$ | $9.6 \pm 1^{*,a}$ $n = 4$ | $-0.7 \pm 0.1^a$ $n = 4$ |
| Branched | 2-Isopropyl ($10^{-10}$–$10^{-4}$ M) | No effect $n = 9$ | No effect $n = 9$ | | | | No effect$^a$ $n = 6$ | | |
| Cyclic | 2-Phenyl ($10^{-11}$–$10^{-6}$ M) | | $86.4 \pm 8^*$ $n = 12$ | $0.04 \pm 0.01^*$ $n = 12$ | | $1.2 \pm 0.1$ $n = 12$ | $-31.1 \pm 2^a$ $n = 7$ | | |
| | 2-Benzyl ($10^{-11}$–$10^{-6}$ M) | | $56.3 \pm 3^*$ $n = 7$ | $0.06 \pm 0.01$ $n = 7$ | | $1.3 \pm 0.1$ $n = 7$ | | $>100^a$ $n = 7$ | |
| | 2-Phenylethyl ($10^{-10}$–$10^{-7}$ M) | No effect $n = 6$ | No effect $n = 6$ | | | | $-30.2 \pm 4^a$ $n = 4$ | | |
| | 2-Cyclohexylmethyl ($10^{-10}$–$10^{-7}$ M) | | $19.3 \pm 4$ $n = 6$ | | | | $-30 \pm 3^a$ $n = 6$ | $>100^a$ $n = 6$ | |

* The data are significantly different from those of the other analogs in the same condition at $P < 0.05$.

channel activation also was observed in 10 mM glucose (Fig. 4C). Partial inhibitory responses of the Kir6.2ΔC36 channel were observed with the 2-cyclic analogs (Table 1).

The application of the 2-$n$-hexyl-1,4-benzoxazine derivative in 3 mM glucose and 5 mM $NaN_3$ induced a dose-dependent cell depolarization that was recorded in the current-clamp mode (Fig. 5B). In 6 mM glucose, this compound also depolarized the cells, but the 2-isopropyl analog was inactive (Fig. 5A). The 2-phenyl analog hyperpolarized the cells at sub-nanomolar concentrations, but it did not cause a significant cell depolarization at higher concentrations (Fig. 5, A and B). The 2-benzyl analog showed approximately 20 mV cell hyperpolarization at sub-nanomolar concentrations (Fig. 5A). The 2-$n$-hexyl analog induced insulin release in vitro, whereas the 2-phenyl analog reduced this insulin release (Fig. 6).
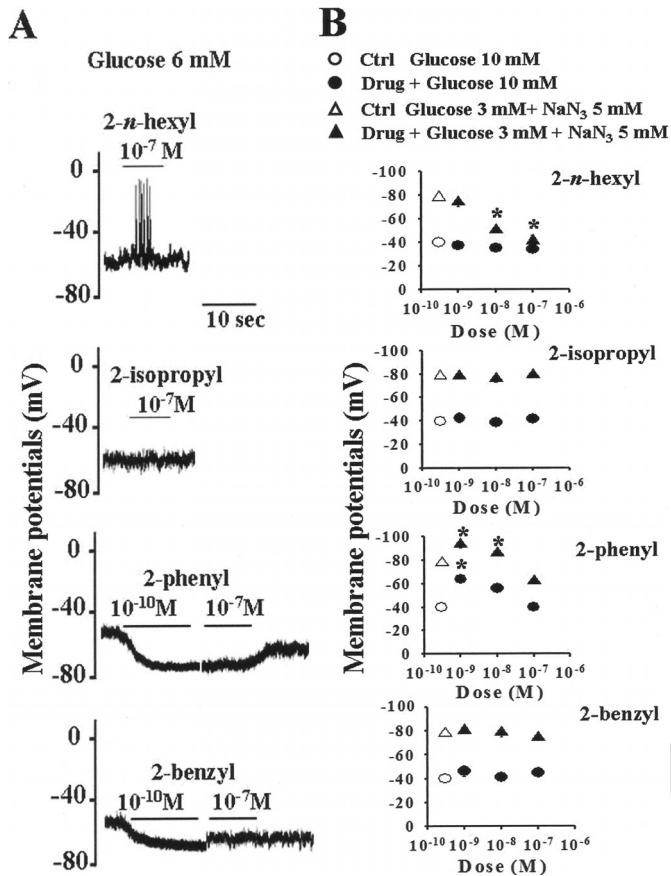
In the excised patch experiments, $10^{-6}$ M of the 2-$n$-hexyl analog caused a channel block of $64 \pm 5\%$ (number of patches = 3) in the presence of ATP and $59 \pm 4\%$ (number of patches = 3) in the absence of the nucleotide. This blocking action was reversed after a 4-s washout. The mean currents were $-30 \pm 1$ pA in the control, $-13.2 \pm 0.4$ pA in the presence of the 2-$n$-hexyl analog ($10^{-6}$ M) and $10^{-4}$ M ATP, $-12.1 \pm 1$ pA in the presence of the 2-$n$-hexyl analog alone ($10^{-6}$ M), $-28 \pm 0.9$ pA after the washout of the drug solution, and $-4.5 \pm 0.3$ pA with $10^{-4}$ M ATP (Fig. 7A). No effects were observed on the single-channel conductances, which were $68 \pm 2$ and $67 \pm 3$ pS (number of patches = 3) in the control and in the presence of a $10^{-6}$ M concentration of the drug, respectively. A $10^{-9}$ M concentration of the 2-phenyl analog led to a channel activation of $59 \pm 4\%$ (number of patches = 3) in the presence of $10^{-4}$ M internal ATP, but it produced a reduction of channel activity at a concentration of $10^{-7}$ M. The mean currents were $-31.5 \pm 1$ pA in the control, $-20.3 \pm 0.4$ pA in the presence of the 2-phenyl analog ($10^{-9}$ M) and $10^{-4}$ M ATP, $-7.1 \pm 0.3$ pA with the 2-phenyl analog ($10^{-7}$ M) and $10^{-4}$ M ATP, $-24.4 \pm 3$ pA after the washout of the drug solution, and $-4.3 \pm 0.4$ pA with $10^{-4}$ M ATP (Fig. 7B).

In the presence of $2 \times 10^{-4}$ M ADP, $10^{-9}$ M of the 2-phenyl analog led to a channel activation of $81 \pm 6\%$ (number of patches = 3) with respect to that of the control, whereas a mild reduction of channel activity was observed at a $10^{-7}$ M concentration (number of patches = 3) (Fig. 7C). The mean currents were $-29.1 \pm 1$ pA in the control, $-36.2 \pm 2$ pA with $2 \times 10^{-4}$ M ADP, $-51 \pm 4$ pA with the 2-phenyl analog ($10^{-9}$ M) and $2 \times 10^{-4}$ M ADP, $-23 \pm 1$ pA with the 2-phenyl analog ($10^{-7}$ M) and $2 \times 10^{-4}$ M ADP, $-25.1 \pm 2$ pA after the washout of the drug solution, and $-3.5 \pm 0.3$ pA with $10^{-4}$ M ATP (Fig. 7C). The 2-isopropyl analog failed to affect the KATP channel in the excised patch experiments (data not shown).

**In Vivo Effects of the 2$H$-1,4-Benzoxazine Derivatives on the Areas under the Curves and Fasting Glucose Levels in Normal Mice.** No macroscopic signs of intolerability were observed in the benzoxazine derivative-treated mice. The mice did not show any type of local reaction after the acute intraperitoneal administration of a single dose of these compounds. No adverse effects were observed at 24 h or 14 days postdose or thereafter.

The in vivo effects of the 2-isopropyl, 2-$n$-hexyl, and 2-phenyl analogs were evaluated by intraperitoneal glucose tolerance test and compared with the effects of glibenclamide or diazoxide. In the control mice that were injected with the vehicle, the administration of 2 g/kg glucose 30 min before the first blood glucose measurement resulted in a typical increase in blood glucose levels from a basal value of $0.86 \pm 0.1$ mg/ml to a peak of $2.72 \pm 0.7$ mg/ml as shown in Fig. 8A. The administration of the 2-$n$-hexyl analog led to a bimodal response in glucose disposal; at a 0.2 mg/kg dose, the blood glucose levels changed from a basal value of $0.6 \pm 0.07$ mg/ml to a peak of $3.31 \pm 0.9$ mg/ml. However, the group injected with 10 mg/kg of the 2-$n$-hexyl analog showed an improvement in the glucose tolerance curve; their blood glucose levels increased from a basal value of $0.66 \pm 0.06$ mg/ml to a peak of $1.64 \pm 0.8$ mg/ml. No significant differences were observed in the peak glucose levels of the mice that were treated with the 2-isopropyl analog with respect to those of the vehicle-
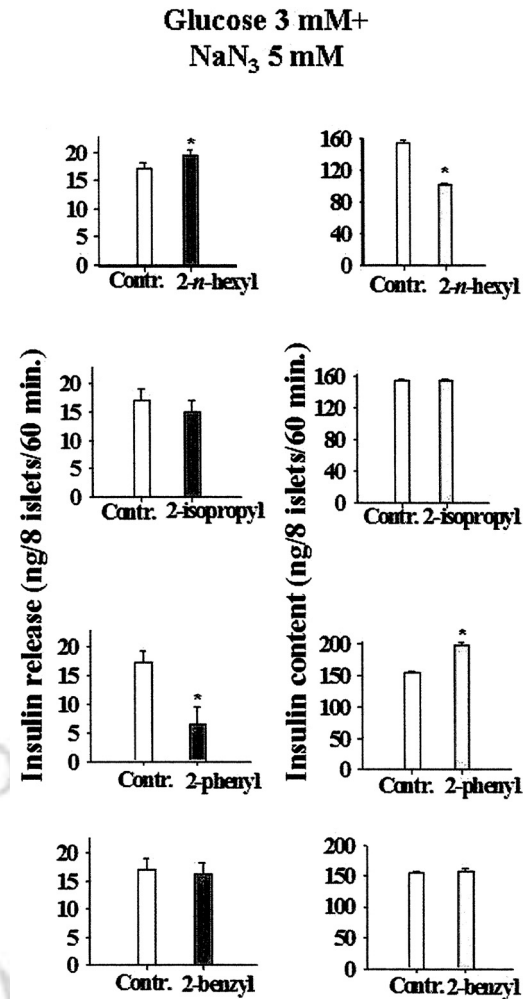
tapraid3/zpt-pt/zpt-pt/zpt00212/zpt9675d12z | xppws | S=1 | 12/30/11 | 18:29 | 4/Color Figure(s): 9 | Art: 185835 | Input-JHG

K$^+$ Channel Modulators and Pancreatic $\beta$ Cells     **7**

**Fig. 4.** Effects of the 2-phenyl-, 2-benzyl-, 2-phenylethyl-, and 2-cyclohexylmethyl-1,4-benzoxazine derivatives on the KATP currents of the pancreatic $\beta$ cells in the presence of 3, 6, or 10 mM glucose. Sample traces of the whole-cell KATP currents were recorded using the perforated patch mode during pulses of $\pm20$ mV (Vm) from a holding potential of $-70$ mV (Vm) in the absence (control, Ctrl) or presence of drugs and at different external glucose concentrations. O indicates the open channel levels as the upward or downward deflections of the current record, and C indicates the closed level. Different concentrations of the same drug are indicated on the corresponding current traces. A, the whole-cell currents that were measured at $-50$ mV (Vm) in 3 mM glucose and 5 mM NaN$_3$ were enhanced with respect to those of the controls after the application of $0.7 \times 10^{-10}$ and $10^{-10}$ M concentrations of the 2-phenyl analog and a $10^{-10}$ M concentration of the 2-benzyl analog. A, a $2.5 \times 10^{-4}$ M concentration of diazoxide (Diazo.) in 3 mM glucose also increased the whole-cell current. A, the concentration-response relationships of the KATP currents versus the 2-phenyl (black triangles), 2-benzyl (black diamonds), 2-phenylethyl (white triangles), and 2-cyclohexylmethyl (upside-down black triangles) analog concentrations constructed in 3 mM glucose and 5 mM NaN$_3$ in the bath at $-50$ mV (Vm) are shown. Each experimental point represents the mean $\pm$ S.E. of the percentage activation of the KATP currents versus the drug concentrations of three cells; no more than two drug concentrations per cell were tested. B, in 6 mM glucose, the whole currents were enhanced after the application of a $10^{-10}$ M concentration of the 2-phenyl and 2-benzyl analogs and by $2.5 \times 10^{-4}$ M diazoxide. C, the average $\beta$ cell KATP current density versus the drug concentrations ($10^{-9}$–$10^{-7}$ M) or diazoxide in 10 mM glucose are shown. Each bar represents the mean $\pm$ S.E. of the current data from three cells. *, these data were significantly different from the controls for $P < 0.05$.

treated mice. The administration of 10 mg/kg of a 2-phenyl analog caused an increase of the glucose level from a basal value of $0.67 \pm 0.06$ mg/ml to a peak of $3.3 \pm 0.9$ mg/ml. A dose of 25 mg/kg diazoxide caused an enhancement of the glucose levels from a basal value of $0.68 \pm 0.08$ mg/ml to a peak of $4.14 \pm 0.4$ mg/ml (Fig. 8A). The animals that were treated with 2 mg/kg glibenclamide showed the most significant improvement in the glucose tolerance curve, with a peak glucose level of $0.89 \pm 0.07$ mg/ml (Fig. 8A).

The administration of increasing doses (0.2, 2, and 10 mg/kg) of the 2-*n*-hexyl analog led to a bimodal response in the area under the curve (AUC) of blood glucose. In fact, at the lower dose of 0.2 mg/kg, the compound significantly increased the AUCs with respect to those of the vehicle; however, at a higher dose of 10 mg/kg, the 2-*n*-hexyl analog significantly decreased the AUC (Table 2). The 2-isopropyl analog increased the AUCs at the higher dose. The glibenclamide treatment (0.2 and 2 mg/kg) significantly decreased the AUCs with respect to those of the vehicle treated-group. The 2-phenyl analog (2–30 mg/kg) increased the AUC in a dose-dependent manner, and diazoxide (25 mg/kg) caused the maximal observed AUC increase (Table 2).

The 2-*n*-hexyl, 2-isopropyl, and 2-phenyl analogs did not significantly affect the fasting blood glucose levels of the mice compared with the 2 mg/kg dose of glibenclamide (Fig. 8B).

## Discussion

In the present work, we showed that the 2-*n*-hexyl-1,4-benzoxazine derivative is a reversible, potent blocker of the KATP channels of native pancreatic $\beta$ cells, which leads to cell depolarization at nanomolar concentrations. Other Kir6.2 blockers that showed glucose-lowering effects exerted their action at micromolar concentrations, and they include the polyamine analogs; the vasodilating iptakalim; the synthetic imidazolines; the antipsychotics haloperidol and olanzapine; the antiarrhythmics cibenzoline, disopyramide, and mexiletine; the antimalarials mefloquine and quinine; and the antibiotics lomefloxacin and gatifloxacin (Bleck et al., 2005; Loussouarn et al., 2005; Zünkler, 2006; Misaki et al., 2007). The 2-*n*-hexyl analog equally blocked the KATP channels of the native $\beta$ cells in the perforated and conventional whole-cell patch clamp methodologies and in the cells that expressed the truncated Kir6.2 subunit in the absence of

**Fig. 5.** Effects of the $2H$-1,4-benzoxazine derivatives on the membrane potential of the pancreatic β cells in different external glucose concentrations. A, time course of the membrane potentials of the pancreatic β cells that were perfused with solutions containing 6 mM glucose in the absence or presence of 2-$n$-hexyl-, 2-isopropyl-, 2-phenyl-, or 2-benzyl-1,4-benzoxazine derivatives at $10^{-10}$ or $10^{-7}$ M concentrations. B, scatter plots of the membrane potentials in the absence (control, Ctrl) or presence of the drugs at different concentrations ($10^{-9}$–$10^{-7}$ M) in 10 or 3 mM glucose and 5 mM $NaN_3$. Each point represents the mean ± S.E. of the absolute values of the voltage data from three cells.
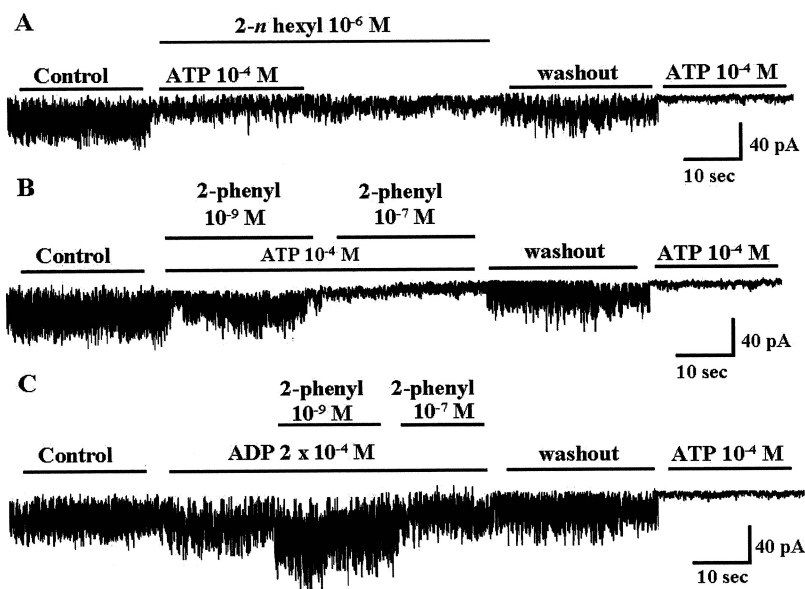
**Fig. 6.** Insulin secretion induced by low external glucose and residual insulin content in the islets. The drug effects on insulin release were evaluated in 3 mM glucose and 5 mM $NaN_3$ and compared with that obtained in the absence of the drugs (Contr.). Batches of eight islets were incubated with the 2-$n$-hexyl ($10^{-8}$ M), 2-isopropyl ($10^{-7}$ M), 2-phenyl ($10^{-9}$ M), and 2-benzyl ($10^{-9}$ M) analogs. Each bar is the mean ± S.E. of three values. ∗, these data are significantly different from the controls for $P < 0.05$.

SURs; these results suggest that the Kir6.2 subunit carries the inhibitory site(s) for this molecule.

The 2-$n$-hexyl analog showed antihyperglycemic activity in the intraperitoneal glucose tolerance test, but it was less effective than glibenclamide. A biphasic behavior was observed in the glucose disposal curves that were determined in vivo after the administration of increasing doses of the 2-$n$-hexyl analog; these data can be explained by accounting for the opposite in vitro effects of this compound on pancreatic β cells and skeletal muscle KATP channels (Fig. 9) (Tricarico et al., 2008).

The 2-phenyl analog activated the pancreatic KATP channels at sub-nanomolar concentrations in the perforated patch-clamp mode; the activation of these channels induces cell hyperpolarization. This activation was more potent but less effective than that of diazoxide. The rank order of potency and efficacy of the channel openers was 2-phenyl > 2-benzyl > 2-cyclohexylmethyl analogs, whereas the 2-phenylethyl analog was not effective. Other pancreatic KCOs that activate the channel at nanomolar concentrations include the thiadiazine-dioxide analogs, such as the NN414, BPDZ-73, 6-chloro-3-(1-methyl-1-phenylethyl)amino-$4H$-thieno[3,2-$e$]-1,2,4-thiadiazine-1,1-dioxide, NNC-55-0462,

and 6-chloro-3-cyclobutylamino-$4H$-1,2,4-benzothiadiazine-1,1-dioxide (Nielsen et al., 2006; Carosati et al., 2007; Judge and Smith, 2009; Fischer et al., 2010; Pirotte et al., 2010).

The actions of the 2-cyclic aromatic analogs were observed mostly in the presence of medium and low glucose concentrations, although they were less effective in the presence of high external glucose concentrations, which suggests that they require a proper ATP/ADP ratio. This hypothesis is confirmed by the fact that in excised patch experiments the 2-phenyl analog is capable of activating the KATP channel in the presence of ATP and ADP. However, the 2-cyclic analogs showed a reduced efficacy in activating the KATP channel currents at a concentration of $>10^{-9}$ M; this concentration can be related to the low-affinity interaction of these molecules with the Kir6.2 subunit. This is supported by the fact that these molecules inhibited the truncated Kir6.2 subunit in the nanomolar concentration range, but they showed a lower efficacy than the 2-linear alkyl chain analog.

As expected for a KATP channel opener, the 2-phenyl analog is the most effective $2H$-1,4-benzoxazine derivative in

tapraid3/zpt-pt/zpt-pt/zpt00212/zpt9675d12z | xppws | S=1 | 12/30/11 | 18:29 | 4/Color Figure(s): 9 | Art: 185835 | Input-JHG

K$^+$ Channel Modulators and Pancreatic $\beta$ Cells **9**

**Fig. 7.** Effects of the 2-$n$-hexyl- and 2-phenyl-1,4-benzoxazine derivatives on the channel currents that were recorded in the excised patches that contained multiple KATP channels from the pancreatic β cells. The KATP channel currents were recorded in excised inside-out patches that were held at −50 mV (Vm) and in the presence of 140 mM KCl on both sides of the membrane. The drug solutions were applied to the internal sides of the patches with or without nucleotides using a fast perfusion system. The 2-$n$-hexyl analog blocks channel currents in the presence and in the absence of internal ATP. A, washout of drug solution rapidly restored channel currents. B and C, the 2-phenyl analog in the presence of the nucleotides increased the channel activity at low concentrations but markedly inhibited it at the high concentration in the presence of internal ATP (B) and caused a mild inhibition of channel activity in the presence of internal ADP (C).
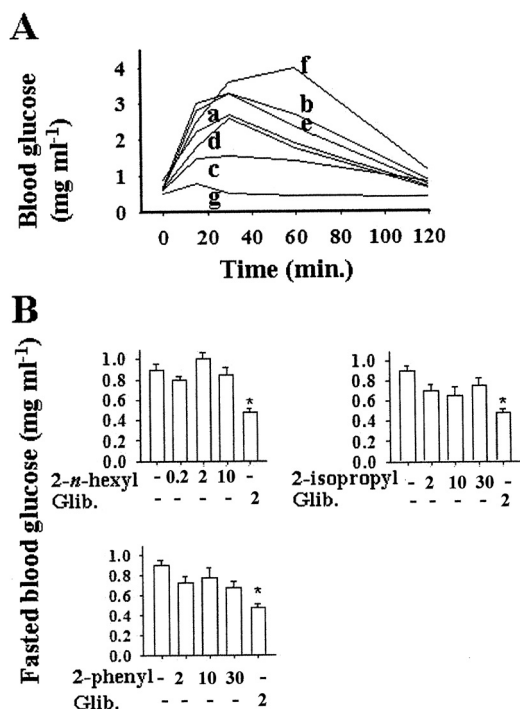


**Fig. 8.** Intraperitoneal glucose tolerance test and fasting glucose levels in the drug-treated mice. A, sample curves representing the blood glucose levels of the mice that fasted for 14 h and then were treated with the vehicle solution (a) or with vehicle solution that was enriched with either 0.2 mg/kg 2-$n$-hexyl (b), 10 mg/kg 2-$n$-hexyl (c), 30 mg/kg 2-isopropyl (d), 10 mg/kg 2-phenyl (e), 25 mg/kg diazoxide (f), or 2 mg/kg glibenclamide (g) are shown. The mice were injected with the drug solutions or vehicle intraperitoneally at a constant volume of 0.15 ml 30 min before glucose loading. The mice were given 2 g/kg glucose via an intraperitoneal injection immediately after the first glycemia determination (time 0). Blood was drawn from a tail vein at 0, 15, 30, 60, and 120 min, and the blood glucose level was measured by the glucose oxidase method (Glucometer Elite; Bayer-Schweiz AG, Zurich, Switzerland). The mean values of the initial ($t = 0$) blood glucose level in the mice that fasted for 14 h and were treated with the vehicle solution; a vehicle solution enriched with either 2-isopropyl-, 2-$n$-hexyl-, or 2-phenyl-1,4-benzoxazine derivatives; or a vehicle solution enriched with glibenclamide (Glib.). B, the tail vein blood sample was taken 30 min after the treatment was administered. ∗, the data were significantly different for $P < 0.05$ with respect to the animal group that was treated with the vehicle.

TABLE 2
AUC data for the serum glucose concentration in the drug-treated mice
The AUC data were obtained during the intraperitoneal glucose tolerance test in the fasted mice that were pretreated with the vehicle solution or the vehicle solution that was enriched with different doses of the $2H$-1,4-benzoxazine derivatives. The AUCs were determined by using the fasting glucose concentration ($t_0$ value) as a reference to minimize the importance of the "starting value."

| | Treatments | Dose | AUC | No. Animals |
|---|---|---|---|---|
| | | $mg/kg$ | $mg \cdot ml^{-1} \cdot min^{-1}$ | |
| Linear | Vehicle | | 217.38 ± 12.41 | 5 |
| | 2-$n$-Hexyl | 0.2 | 413.38 ± 39.39* | 4 |
| | | 2 | 270.34 ± 36.44 | 5 |
| | | 10 | 150.64 ± 23.04* | 4 |
| Branched | 2-Isopropyl | 2 | 197.85 ± 45.22 | 3 |
| | | 10 | 238.88 ± 51.27 | 3 |
| | | 30 | 259.58 ± 38.82* | 4 |
| Cyclic | 2-Phenyl | 2 | 256.36 ± 43.26 | 3 |
| | | 10 | 339.03 ± 27.62* | 5 |
| | | 30 | 393.03 ± 31.31* | 5 |
| | Glibenclamide | 0.2 | 128.08 ± 15.44* | 4 |
| | | 2 | 103.23 ± 25.41* | 3 |
| | Diazoxide | 25 | 450.80 ± 59.78* | 3 |

* The data were significantly different for $P < 0.05$ with respect to the animal group that was treated with the vehicle.

increasing the AUC in normal mice, and this effect is similar to that of diazoxide; however, diazoxide caused the maximal observed increase of the AUC.

The introduction of a branched alkyl chain at position 2 of the $2H$-1,4-benzoxazione nucleus leads to the formation of an inactive compound on the pancreatic KATP channel, as in the case of the 2-isopropyl analog; however, this analog is effective on the skeletal muscle subtype (Tricarico et al., 2008).

The 2-isopropyl analog induced a dose-dependent enhancement of the AUC of blood glucose; this result can be related to the activating action of the skeletal muscle KATP channels (Fig. 9).

Although glibenclamide affected the fasting blood glucose levels of the normal mice, the 2-$n$-hexyl-, 2-phenyl-, and 2-isopropyl-1,4-benzoxazine derivatives did not affect the fasting blood glucose levels of these mice. These compounds did not affect the fasting glucose levels with respect to those of glibenclamide because of their different modes of action on the target tissues. For example, the decrease of blood glucose

**C O L O R**
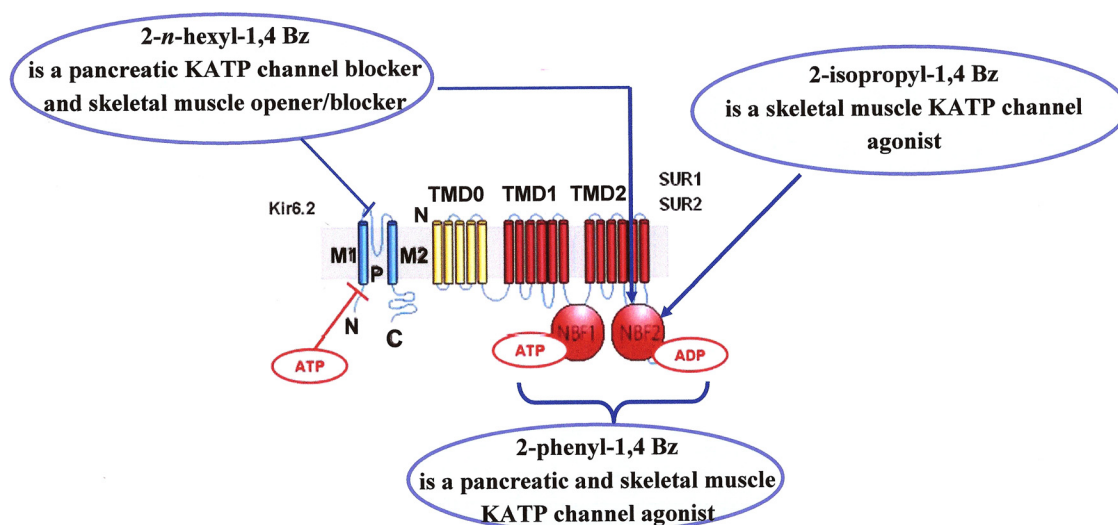


**Fig. 9.** Hypothetical binding sites of the 2*H*-1,4-benzoxazine derivatives on the Kir6.2 subunit and SUR1 or SUR2. The 2-hexyl analog preferentially binds to the ATP sites of the Kir6.2 subunit and exerts its blocking action in the pancreatic β cells and the skeletal muscles. This chemical showed an opening action in the skeletal muscle through its interaction with NBF2 of SUR2A. The 2-isopropyl analog is a KATP channel agonist that interacts with the unique residues that are located in NBF2 of SUR2A. The 2-phenyl analog activates both the pancreatic β cells and the skeletal muscle KATP channels by possibly interacting with NBF2 of SUR2A and NBF1 of SUR1.

due to the insulinotropic effect of the 2-*n*-hexyl analog is somehow counterbalanced by the KCO action on the skeletal muscle subtype. The actions of these drugs on neuronal KATP channels also should be considered. This specific channel controls the electrical activity of many types of neurons that are sensitive to the glucose level, thereby influencing glucose homeostasis. For example, a reduction in extracellular glucose causes the opening of the KATP channels in glucose-sensitive neurons of the ventromedial hypothalamus, which triggers adrenaline-dependent glucagon secretion and the counterregulatory response to hypoglycemia. The KATP channel activation, which is sufficient to abolish the electrical activity of the pro-opiomelanocortin-expressing neurons in the arcuate nucleus, leads to hyperphagia and increased body weight. Their partial activation, which reduces but does not abolish electrical activity, prevents glucose sensing and leads to impaired glucose tolerance (McTaggart et al., 2010). The differences in the kinetics of the actions of these compounds, which are rapidly reversible with the linear alkyl chain derivative compared with the sulfonylurea compound, also may play a role.

In conclusion, the 2-linear alkyl chain is the molecular determinant that confers the blocking action to the 2*H*-1,4-benzoxazines in pancreatic β cells, whereas the branched substituent is the molecular determinant that confers the activating action in skeletal muscles. The aromatic substituent confers the opening action to the 2*H*-1,4-benzoxazines in both the pancreatic β cells and the skeletal muscle cells. SUR1 shows an overall identity of 79% with SUR2A; larger differences exist in the amino acid sequences of the first nucleotide binding fold-2 (NBF2) and second transmembrane domain (TMD2) regions, and additional minor differences were found in the NBF2 region (Moreau et al., 2005). The NBF2 region confers sensitivity to the SUR2 openers with a benzopyran-like structure (cromakalim) and the pyridine (pinacidil) (Moreau et al., 2005). We propose that 2-isopropyl-1,4-benzoxazine, which is a structurally related analog of nucleotides, can bind to a site that is located on the NBF2 of

SUR2A, although its interaction with TMD2 cannot be excluded. The 2-*n*-hexyl analog blocks the pancreatic and skeletal muscle KATP channels by interacting with the Kir6.2 subunit, but it also activates the muscle KATP channel by potentially interacting with the TMD2-NBF2 region. 2-Phenyl-1,4-benzoxazine activates both the pancreatic β cells and the skeletal muscle channels with a comparable potency and efficacy. These actions can be mediated by the binding of a drug to the TMD2-NBF2 region and to an additional site located on TMD1-NBF1, which is the main region that is responsible for the binding and activation of the pancreatic β cell KATP channel by diazoxide (Babenko et al., 2000; Moreau et al., 2005) (Fig. 9).

The 2-*n*-hexyl analog action that is mediated by the Kir6.2 subunit is an alternative mechanism of action with respect to that of the hypoglycemic sulfonylureas that target SUR1. This can be related to the structural similarity of this compound with the ATP molecule (Tricarico et al., 2008). The 2-phenyl analog may represent a potential drug treatment in patients who are intolerant to diazoxide. The 2*H*-1,4-benzoxazines have a differential pharmacological profile with respect to those of the SUR1 blockers or openers; in vitro and in vivo, they show a combined activating/blocking action toward KATP channels that confers significant glycemic control after the administration of a glucose bolus, but they do not affect fasting glycemia. In addition, their opening action of the skeletal muscle KATP channels may be cytoprotective, although pure SUR2A openers may lead to arrhythmia (Jahangir and Terzic, 2005). A similar mechanism has been proposed for iptakalim, which is a potent sub-nanomolar vascular KATP channel opener. At a high micromolar concentration, iptakalim shows a blocking action of the pancreatic channel, and it is in clinical development as an antihypertensive drug (Misaki et al., 2007; Pan et al., 2010).

**AQ: G**  **Authorship Contributions**

*Participated in research design:* Tricarico and Rolland.

*Conducted experiments:* Rolland, Cannone, Mele, and Cippone.

*Contributed new reagents or analytic tools:* Laghezza, Carbonara, Fracchiolla, Tortorella, and Loiodice.

*Performed data analysis:* Cannone and Mele.

*Wrote or contributed to the writing of the manuscript:* Tricarico, Mele, and Conte Camerino.

### References

Arnoux JB, de Lonlay P, Ribeiro MJ, Hussain K, Blankenstein O, Mohnike K, Valayannopoulos V, Robert JJ, Rahier J, Sempoux C, et al. (2010) Congenital hyperinsulinism. *Early Hum Dev* **86:**287–294.

Ashcroft FM (2010) New uses for old drugs: neonatal diabetes and sulphonylureas. *Cell Metab* **11:**179–181.

Babenko AP, Gonzalez G, and Bryan J (2000) Pharmaco-topology of sulfonylurea receptors. Separate domains of the regulatory subunits of K(ATP) channel isoforms are required for selective interaction with K(+) channel openers. *J Biol Chem* **275:**717–720.

Bleck C, Wienbergen A, and Rustenbeck I (2005) Essential role of the imidazoline moiety in the insulinotropic effect but not the KATP channel-blocking effect of imidazolines; a comparison of the effects of efaroxan and its imidazole analogue, KU14R. *Diabetologia* **48:**2567–2575.

Carosati E, Mannhold R, Wahl P, Hansen JB, Fremming T, Zamora I, Cianchetta G, and Baroni M (2007) Virtual screening for novel openers of pancreatic K(ATP) channels. *J Med Chem* **50:**2117–2126.

Fischer A, Schmidt C, Lachenicht S, Grittner D, Winkler M, Wrobel T, Rood A, Lemoine H, Frank W, and Braun M (2010) Synthesis of benzofuran, benzothiophene, and benzothiazole-based thioamides and their evaluation as K(ATP) channel openers. *ChemMedChem* **5:**1749–1759.

Flanagan SE, Patch AM, Mackay DJ, Edghill EL, Gloyn AL, Robinson D, Shield JP, Temple K, Ellard S, and Hattersley AT (2007) Mutations in ATP-sensitive K+ channel genes cause transient neonatal diabetes and permanent diabetes in childhood or adulthood. *Diabetes* **56:**1930–1937.

Flechtner I, de Lonlay P, and Polak M (2006) Diabetes and hypoglycaemia in young children and mutations in the Kir6.2 subunit of the potassium channel: therapeutic consequences. *Diabetes Metab* **6:**569–580.

Gribble FM and Reimann F (2003) Sulphonylurea action revisited: the post-cloning era. *Diabetologia* **46:**875–891.

Hambrock A, de Oliveira Franz CB, Hiller S, and Osswald H (2006) Glibenclamide-induced apoptosis is specifically enhanced by expression of the sulfonylurea receptor isoform SUR1 but not by expression of SUR2B or the mutant SUR1(M1289T). *J Pharmacol Exp Ther* **316:**1031–1037.

Hansen JB (2006) Towards selective Kir6.2/SUR1 potassium channel openers, medicinal chemistry and therapeutic perspectives. *Curr Med Chem* **13:**361–376.

Hussain K (2007) Insights in congenital hyperinsulinism. *Endocr Dev* **11:**106–121.

Jahangir A and Terzic A (2005) K(ATP) channel therapeutics at the bedside. *J Mol Cell Cardiol* **39:**99–112.

Judge SI and Smith PJ (2009) Patents related to therapeutic activation of K(ATP) and K(2P) potassium channels for neuroprotection: ischemic/hypoxic/anoxic injury and general anesthetics. *Expert Opin Ther Pat* **19:**433–460.

Koster JC, Permutt MA, and Nichols CG (2005) Diabetes and insulin secretion: the ATP-sensitive K+ channel (K ATP) connection. *Diabetes* **54:**3065–3072.

Loussouarn G, Marton LJ, and Nichols CG (2005) Molecular basis of inward rectification: structural features of the blocker defined by extended polyamine analogs. *Mol Pharmacol* **68:**298–304.

Maedler K, Carr RD, Bosco D, Zuellig RA, Berney T, and Donath MY (2005) Sulfonylurea induced beta-cell apoptosis in cultured human islets. *J Clin Endocrinol Metab* **90:**501–506.

McTaggart JS, Clark RH, and Ashcroft FM (2010) The role of the KATP channel in glucose homeostasis in health and disease: more than meets the islet. *J Physiol* **588:**3201–3209.

Misaki N, Mao X, Lin YF, Suga S, Li GH, Liu Q, Chang Y, Wang H, Wakui M, and Wu J (2007) Iptakalim, a vascular ATP-sensitive potassium (KATP) channel opener, closes rat pancreatic beta-cell KATP channels and increases insulin release. *J Pharmacol Exp Ther* **322:**871–878.

Mlynarski W, Tarasov AI, Gach A, Girard CA, Pietrzak I, Zubcevic L, Kusmierek J, Klupa T, Malecki MT, and Ashcroft FM (2007) Sulfonylurea improves CNS function in a case of intermediate DEND syndrome caused by a mutation in KCNJ11. *Nat Clin Pract Neurol* **3:**640–645.

Moreau C, Prost AL, Dérand R, and Vivaudou M (2005) SUR, ABC proteins targeted by KATP channel openers. *J Mol Cell Cardiol* **38:**951–963.

Nielsen FE, Ebdrup S, Jensen AF, Ynddal L, Bodvarsdottir TB, Stidsen C, Worsaae A, Boonen HC, Arkhammar PO, Fremming T, et al. (2006) New 3-alkylamino-4H-thieno-1,2,4-thiadiazine 1,1-dioxide derivatives activate ATP-sensitive potassium channels of pancreatic beta cells. *J Med Chem* **49:**4127–4139.

Nourparvar A, Bulotta A, Di Mario U, and Perfetti R (2004) Novel strategies for the pharmacological management of type 2 diabetes. *Trends Pharmacol Sci* **25:**86–91.

Pan Z, Huang J, Cui W, Long C, Zhang Y, and Wang H (2010) Targeting hypertension with a new adenosine triphosphate-sensitive potassium channel opener iptakalim. *J Cardiovasc Pharmacol* **56:**215–228.

Pearson ER, Flechtner I, Njølstad PR, Malecki MT, Flanagan SE, Larkin B, Ashcroft FM, Klimes I, Codner E, Iotova V, et al. (2006) Switching from insulin to oral sulfonylureas in patients with diabetes due to Kir6.2 mutations. *N Engl J Med* **355:**467–477.

Pirotte B, de Tullio P, Nguyen QA, Somers F, Fraikin P, Florence X, Wahl P, Hansen JB, and Lebrun P (2010) Chloro-substituted 3-alkylamino-4H-1,2,4-benzothiadiazine 1,1-dioxides as ATP-sensitive potassium channel activators: impact of the position of the chlorine atom on the aromatic ring on activity and tissue selectivity. *J Med Chem* **53:**147–154.

Rolland JF, Henquin JC, and Gilon P (2002) Feedback control of the ATP-sensitive K(+) current by cytosolic Ca(2+) contributes to oscillations of the membrane potential in pancreatic beta-cells. *Diabetes* **51:**376–384.

Rolland JF, Tricarico D, Laghezza A, Loiodice F, Tortorella V, and Camerino DC (2006) A new benzoxazine compound blocks KATP channels in pancreatic beta cells: molecular basis for tissue selectivity in vitro and hypoglycaemic action in vivo. *Br J Pharmacol* **149:**870–879.

Seino S and Miki T (2003) Physiological and pathophysiological roles of ATP-sensitive K+ channels. *Prog Biophys Mol Biol* **81:**133–176.

Simard JM, Woo SK, Bhatta S, and Gerzanich V (2008) Drugs acting on SUR1 to treat CNS ischemia and trauma. *Curr Opin Pharmacol* **8:**42–49.

Takahashi A, Nagashima K, Hamasaki A, Kuwamura N, Kawasaki Y, Ikeda H, Yamada Y, Inagaki N, and Seino Y (2007) Sulfonylurea and glinide reduce insulin content, functional expression of K(ATP) channels, and accelerate apoptotic beta-cell death in the chronic phase. *Diabetes Res Clin Pract* **77:**343–350.

Teshima Y, Akao M, Li RA, Chong TH, Baumgartner WA, Johnston MV, and Marbán E (2003) Mitochondrial ATP-sensitive potassium channel activation protects cerebellar granule neurons from apoptosis induced by oxidative stress. *Stroke* **34:**1796–1802.

Tricarico D, Barbieri M, Antonio L, Tortorella P, Loiodice F, and Camerino DC (2003) Dualistic actions of cromakalim and new potent 2H-1,4-benzoxazine derivatives on the native skeletal muscle K ATP channel. *Br J Pharmacol* **139:**255–262.

Tricarico D, Mele A, Camerino GM, Bottinelli R, Brocca L, Frigeri A, Svelto M, George AL Jr, and Camerino DC (2010) The KATP channel is a molecular sensor of atrophy in skeletal muscle. *J Physiol* **588:**773–784.

Tricarico D, Mele A, Camerino GM, Laghezza A, Carbonara G, Fracchiolla G, Tortorella P, Loiodice F, and Camerino DC (2008) Molecular determinants for the activating/blocking actions of the 2H-1,4-benzoxazine derivatives, a class of potassium channel modulators targeting the skeletal muscle KATP channels. *Mol Pharmacol* **74:**50–58.

Zünkler BJ (2006) Human ether-a-go-go-related (HERG) gene and ATP-sensitive potassium channels as targets for adverse drug effects. *Pharmacol Ther* **112:**12–37.

**Address correspondence to:** Domenico Tricarico, Department of Pharmacobiology, Faculty of Pharmacy, University of Bari, Via Orabona No. 4, I-70126 Bari, Italy. E-mail address: dtricarico@farmbiol.uniba.it   **AQ: H**